

Electron transfer into the $n = 3$ states of hydrogen by proton impact on gases*

H. R. Dawson and D. H. Loyd

Department of Physics, Angelo State University, San Angelo, Texas 76901

(Received 18 June 1976)

Absolute cross sections for electron transfer into the $3p$ and $3d$ states of hydrogen have been measured for 2.2- to 8.2-keV proton impact on He, Ar, Kr, O₂, H₂, and N₂. An apparent maximum occurs in the $3d$ cross section for both Ar and H₂. Balmer-alpha cross sections are synthesized from these results and previously reported $3s$ cross sections.

INTRODUCTION

Cross-section measurements for electron transfer into the $3s$ and $4s$ states of H by fast-proton impact on N₂, O₂, H₂, Ar, He, and Kr have been reported by this and other laboratories.¹⁻⁴ Cross sections for transfer into the $3p$ and $3d$ states in the range of impact energies from 2 to 100 keV have also been reported for fast-proton impact on N₂, O₂, H₂, Ar, and He.⁵⁻⁷ This paper reports cross-section measurements for $3p$ and $3d$ transfer due to fast-proton impact on N₂, O₂, H₂, Ar, He, and Kr at energies less than 8.2 keV. A synthesized total Balmer-alpha ($n = 3 \rightarrow 2$) cross section from these data is compared to measurements by other investigators.^{5,6,8,9}

The technique used to measure the $3p$ and $3d$ cross sections is the same as that described in Refs. 5 and 6 and can be summarized as follows. A highly collimated beam of monoenergetic protons entered a differentially pumped collision chamber, containing the target gas, where electron transfer took place. The partially neutralized beam which contained atomic hydrogen in various states of excitation, then passed into an evacuated observation chamber. Balmer-alpha radiation intensity was measured at points along the observation chamber.

If the pressure in the collision chamber is low enough so that only single collision events occur and cascade is neglected, then the excited-atom density in each state at a distance x into the observation chamber is given by an expression of the form

$$n^* = ne^{-x/v\tau}, \quad (1)$$

where v is the atom velocity, τ is the state lifetime, and n is the excited-hydrogen-atom density in that state at $x = 0$. The value of n is determined by $n = F\rho\sigma\tau(1 - e^{-L/v\tau})$ where F is the average proton flux, ρ is the collision-chamber gas density, σ is the cross section for transfer into the state, and L is the collision-chamber length.

Combining expressions of the form of Eq. (1) for each of the three states ($3s$, $3p$, and $3d$) and including the transition probability for the Balmer-alpha transition from each state, leads to an expression for N , the number of Balmer-alpha photons per sec per cm³ emitted from a point at a distance x ,

$$N = n_{3p} A_{3p} e^{-x/v\tau_{3p}} + n_{3d} A_{3d} e^{-x/v\tau_{3d}} + n_{3s} A_{3s} e^{-x/v\tau_{3s}}, \quad (2)$$

where A_{3p} , A_{3d} , and A_{3s} represent the transition probabilities for the transitions $3p \rightarrow 2s$, $3d \rightarrow 2p$, and $3s \rightarrow 2p$, respectively.

Since the $3p$, $3d$, and $3s$ state lifetimes differ greatly, it is possible to resolve the Balmer-alpha radiation into these separate decays with the proper theoretical lifetimes. Additional measurements of target gas pressure and proton flux and utilization of the transfer cross sections for the $3s$ state from Refs. 3 and 4 then allow the transfer cross sections for the $3p$ and $3d$ states to be determined.

APPARATUS

The apparatus used was exactly as described in Ref. 3 with the following exceptions. A precollimation aperture was placed in front of the collision chamber to reduce the amount of beam striking the $\frac{1}{16}$ -in.-diam exit aperture. Significant amounts of beam striking this aperture could create electric fields due to charging of the surface around the aperture. Creation of significant electric fields in the region of the beam could cause Stark mixing of the states.⁵

One factor upon which the relative populations of the $3p$, $3d$, and $3s$ states depend is the length of the collision chamber. The length of the collision chamber was reduced from 7 to 3.5 cm to enhance the population of the $3p$ and $3d$ states relative to the $3s$ state.

A third modification was the reduction of the mask on the photomultiplier tube so that only a

0.5-cm length of beam was viewed through the unit magnification optical system. Since the relative intensity of the Balmer-alpha radiation initially decreases very rapidly as a function of distance from the aperture, the smaller mask produced better resolution in this region.

PROCEDURE

With the gas pressure in the collision chamber fixed, the Balmer-alpha radiation intensity per unit beam current was measured at 1-cm intervals along the beam in the observation chamber. Each measurement included a 0.5-cm segment of the beam. Measurements extended from the exit aperture to a distance where essentially all Balmer-alpha radiation was from the 3s state. This procedure was repeated for each energy investigated.

Collision-chamber pressures were kept low enough to assure single-collision events. The radiation intensity always showed linearity with pressure and beam current.

A background correction was necessary owing to the production of Balmer-alpha radiation by collisions inside the observation chamber. The correction was made in the following manner. The collision chamber was opened to the low-pressure region of the apparatus by means of a valve, and target gas was admitted into the observation chamber at a point near the exit aperture. Gas flow was adjusted until the pressure inside the observation chamber was the same as that during the data run. The pressure was typically 2% of the collision-chamber pressure. Measurements of radiation intensity were made in the same manner as for a data run, and this contribution was subtracted from the data-run measurements.

The resulting Balmer-alpha decay curves were analyzed in the following manner. All background corrected curves for a given reaction at a particular energy were normalized and averaged. This process yielded a standard deviation for each point

which is a measure of the reproducibility of the data runs. The average decay curve was then normalized and plotted.

Since the slope of the decay from each component transition in the Balmer-alpha intensity is known from the state lifetime, only the intercept for each state must be determined. The process used for the determination of the intercepts was as follows. A 3s intercept was chosen which gave the best fit to the original decay curve in the region where essentially all the contribution was from the 160-nsec-lifetime 3s state. This contribution from the 3s state was subtracted from the original curve with no uncertainty assumed in this subtraction. The remaining curve, containing the 15.6-nsec-lifetime 3d-state and 5.4-nsec-lifetime 3p-state contributions, was then plotted using the uncertainties in the data points from the original curve as the uncertainty in the remaining curve. A determination of the 3d intercept and the uncertainty in the 3d intercept was made in the following manner. Maximum and minimum reasonable values of 3d intercept (consistent with the uncertainties) were chosen to fit the remaining curve in the region where essentially all the contribution was from the 15.6-nsec-lifetime 3d state. The 3d cross section was determined using a value for the 3d intercept that was the average of these two intercepts, and the uncertainty in the cross section was determined from half the difference between the two intercepts. Since the sum of the 3s, 3p, and 3d intercepts must be unity for these normalized curves, the above process also determines the 3p intercept which in turn determines the 3p cross section.

From the analysis the intercepts I_{3s}, I_{3p}, I_{3d} of the three decay components at $x = 0$ were determined. These intercepts are the coefficients of the terms in Eq. (2). Since the 3s cross section is known, it is convenient to determine the 3p and 3d cross sections in terms of the 3s cross section.^{3,4} The equation that results for the 3p cross section is

TABLE I. Cross sections in units of 10^{-19} cm².

H ⁺ energy ^a (keV)	Hydrogen		Nitrogen		Oxygen	
	3p	3d	3p	3d	3p	3d
2.2	12 ± 12	8.7 ± 1.0				
2.7					80 ± 45	15.4 ± 4.0
3.2	25 ± 11	10.2 ± 1.0	140 ± 140	43 ± 12	25 ± 25	28.3 ± 2.2
4.2	36 ± 28	8.7 ± 2.7	110 ± 79		29 ± 29	33.5 ± 2.8
4.2	40 ± 17	6.4 ± 1.6	62 ± 62	37 ± 6	20 ± 20	34.8 ± 1.9
5.2	42 ± 24	10.0 ± 2.3	65 ± 65	40 ± 7	110 ± 110	30 ± 12
6.2	29 ± 19	8.4 ± 2.0	120 ± 54	33 ± 9	75 ± 34	32.1 ± 3.5
7.2	34 ± 21	9.4 ± 2.3	165 ± 65	27 ± 7	91 ± 91	26 ± 10
8.2	14 ± 14	14.3 ± 1.5	147 ± 37	25 ± 6	71 ± 44	26.6 ± 5.0

^aDeuteron data listed at proton energy having same particle velocity as deuteron energy used. All deuteron data are contained in the first four rows of this table.

TABLE II. Cross sections in units of 10^{-19} cm².

H ⁺ energy ^a (keV)	Argon		Helium		Krypton	
	3p	3d	3p	3d	3p	3d
3.2	92 ± 92	30.0 ± 8.1	3.7 ± 2.9	1.35 ± 0.36		
4.2	85 ± 65	24.4 ± 6.2	4.6 ± 3.4	1.13 ± 0.30	61 ± 61	21.9 ± 5.8
4.2	48 ± 48	23.8 ± 4.6			71 ± 58	25.8 ± 5.5
5.2	107 ± 63	19.3 ± 6.4			158 ± 41	12.5 ± 4.1
6.2	84 ± 56	35.0 ± 6.0	7.7 ± 2.8	1.22 ± 0.29	84 ± 70	31.1 ± 7.3
7.2	74 ± 30	31.5 ± 3.3	3.4 ± 3.4	1.74 ± 0.37	153 ± 65	35.2 ± 7.2
8.2	122 ± 56	29.5 ± 6.5	13.7 ± 6.8	1.69 ± 0.65	131 ± 87	45.7 ± 9.9

^aDeuteron data listed at proton energy having same velocity as deuteron energy used. All deuteron data are contained in the first two rows of this table.

$$\sigma_{3p} = \sigma_{3s} \frac{I_{3p}(\tau_{3s})^2 [1 - \exp(-D/v\tau_{3s})] [1 - \exp(-L/v\tau_{3s})] A_{3s}}{I_{3s}(\tau_{3p})^2 [1 - \exp(-D/v\tau_{3p})] [1 - \exp(-L/v\tau_{3p})] A_{3p}} \quad (3)$$

where D is the length of beam sampled. The equation is explicitly shown here to point out that the measurements are independent of the actual values of gas density and proton flux provided they are constant. An analogous equation can be written for σ_{3d} by replacing all $3p$ terms in Eq. (3) with $3d$ terms.

Polarization of the radiation from the $3p$ and $3d$ states should require corrections to the σ_{3p} and σ_{3d} values determined by the above equations.^{5,6} Attempts were made to determine the polarization, but the results were so uncertain that no reliable statement about the polarization could be made from them. The uncertainty in the polarization is large because the technique depends on determining small differences between signals which are themselves very small. Therefore no corrections have been made for polarization effects for any of the data.

RESULTS AND DISCUSSION

The results for the $3p$ and $3d$ cross sections are listed in Tables I and II. Table III is a listing of total Balmer-alpha cross sections (transfer into the $n=3$ state) synthesized from the data of Tables I and II and previously reported $3s$ cross sections.^{3,4}

Figures 1 and 2 show log-log plots of the present measurements of the $3p$ and $3d$ cross sections versus energy for proton and deuteron impact of the six target gases. Also shown are previous measurements by other investigators.^{6,7} The error bars shown indicate the uncertainty in the measurements as determined by the method described in the previous section. Uncertainties in the $3p$ cross sections are generally much larger than the uncertainties in the $3d$ cross sections. The reason for this is that in the analysis the un-

TABLE III. Cross sections for total Balmer-alpha in units of 10^{-19} cm².

H ⁺ energy ^a (keV)	Hydrogen	Nitrogen	Oxygen	Argon	Helium	Krypton
2.2	15.7 ± 3.2					
3.2	21.2 ± 2.9	93 ± 29	67 ± 13	65 ± 20	3.09 ± 0.77	
4.2	20.8 ± 5.2	81 ± 14	77 ± 10	63 ± 11	3.15 ± 0.78	67 ± 14
5.2	25.5 ± 5.2	83 ± 15	92 ± 32	69 ± 15		68 ± 10
6.2	23.7 ± 5.1	85 ± 16	84 ± 10	83 ± 14	4.18 ± 0.73	70 ± 16
7.2	26.8 ± 5.6	85 ± 15	81 ± 27	79 ± 8	4.46 ± 0.77	98 ± 16
8.2	31.9 ± 3.2	85 ± 11	83 ± 13	70 ± 17	6.1 ± 1.6	112 ± 22

^aDeuteron data listed at proton energy having same particle velocity as deuteron energy used. All deuteron data are contained in the first three rows of this table.

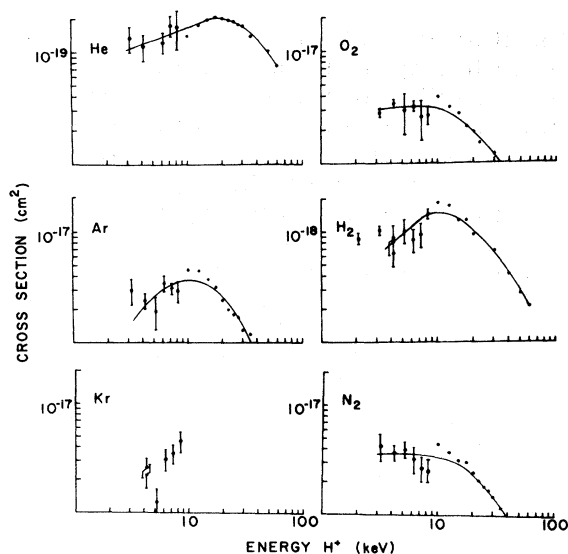


FIG. 1. Plot of $3d$ transfer by H^+ and D^+ on He, Ar, Kr, O_2 , H_2 , and N_2 from Tables I and II. Points without error bars represent data from Ref. 6. Solid lines are smooth curves drawn through the data points.

certainties in the $3p$ and $3d$ cross sections were coupled. Thus for a given energy, the $3p$ and $3d$ intercepts had the same absolute uncertainty. Since the $3p$ intercepts were generally much smaller than the $3d$ intercepts, the resulting relative uncertainties in the $3p$ cross sections were larger

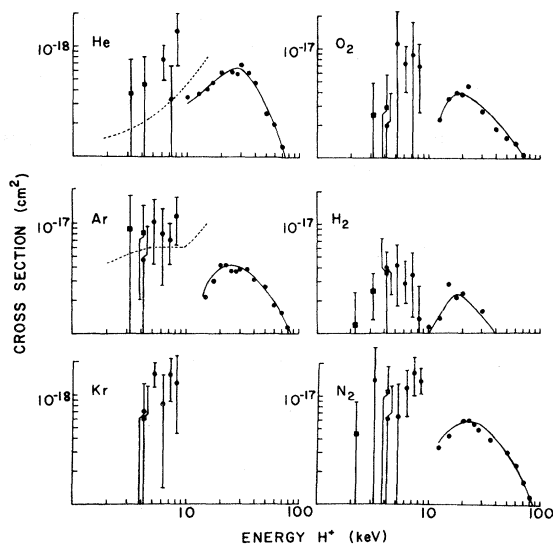


FIG. 2. Plot of $3p$ transfer by H^+ and D^+ on He, Ar, Kr, O_2 , H_2 , and N_2 from Tables I and II. Points without error bars represent data from Ref. 6. Dashed line represents data from Ref. 7. Solid lines are smooth curves drawn through the data points.

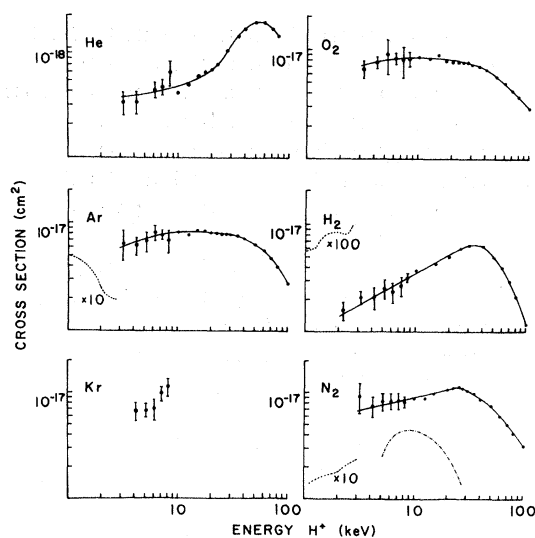


FIG. 3. Plot of Balmer- α cross sections due to H^+ and D^+ impact on He, Ar, Kr, O_2 , H_2 , and N_2 from Table III. Points without error bars represent data from Ref. 6. The dot-dash curve represents data from Ref. 8. Data from Ref. 9 are shown by dashed curve. Solid lines are smooth curves drawn through the data points.

than the relative uncertainties in the $3d$ cross sections. Unfortunately, in some instances the uncertainty in the $3p$ cross section is as large as the measurement. These data may serve only to indicate an upper limit on the cross section.

Figure 1 shows that the $3d$ cross-section data of the present experiment join smoothly with previous data of Hughes *et al.*⁶ at higher energy. The solid line represents a smooth curve drawn through the data points and has no theoretical basis.

The previous data of Hughes *et al.*⁶ had established a maximum in the $3d$ cross section for He at about 20 keV, and the present data indicate no additional structure in the cross section as a function of energy. Considering both the present data and prior data, a maximum in the cross section as a function energy is indicated around 10 keV for both Ar and H_2 . No maximum appears in the O_2 or N_2 cross sections, but instead these cross sections become relatively constant in the energy region below 10 keV.

Figure 2 shows that the present measurements of the $3p$ cross section for He and Ar agree within the uncertainties with recent measurements of these cross sections by Risley, de Heer, and Kerkdijk,⁷ although their data points consistently lie somewhat below the present results. The results of Ref. 6 for He join smoothly with the present results within the uncertainties, although their data lie even lower than that of Ref. 7. The re-

sults of $3p$ cross section measurements by Hughes *et al.*⁶ for Ar, O₂, H₂, and N₂ at higher energies fail to join smoothly with any of the measurements at lower energy. With the possible exception of O₂, their data appear to have the right shape to join smoothly with the low-energy data if their data were increased in magnitude by approximately a factor of 5.

Figure 3 shows log-log plots of the Balmer-alpha cross section synthesized from the $3s$, $3p$, and $3d$ cross sections measured in this laboratory. The equation used for this synthesis was

$$\sigma_{\alpha} = \sigma_s + 0.118\sigma_p + \sigma_d. \quad (4)$$

The coefficients are the branching ratios for the $n=3$ to $n=2$ level.

Also shown in Fig. 3 are measurements of these cross sections by several other laboratories.^{6,8,9} There is excellent agreement between the present results and those of Ref. 6. The results of Hess⁹ have been multiplied by a factor of 10 or 100 in order to even place them on the graph which indicates the total lack of agreement between their results and other measurements. The results of Ref. 8 are of the same order of magnitude of those of Ref. 6 and the results from the present experiment.

ACKNOWLEDGMENTS

We wish to thank David Gressett and Patrick Moore for their able assistance in the data collection.

*Research supported by the Robert A. Welch Foundation.

¹R. H. Hughes, H. R. Dawson, and B. M. Doughty, *Phys. Rev.* **164**, 166 (1967).

²R. H. Hughes, H. R. Dawson, B. M. Doughty, D. B. Kay, and C. A. Stigers, *Phys. Rev.* **146**, 53 (1966).

³H. R. Dawson and D. H. Loyd, *Phys. Rev. A* **9**, 166 (1974).

⁴D. H. Loyd and H. R. Dawson, *Phys. Rev. A* **11**, 140 (1975).

⁵R. H. Hughes, B. M. Doughty, and A. R. Filipelli, *Phys. Rev.* **173**, 172 (1968).

⁶R. H. Hughes, C. A. Stigers, B. M. Doughty, and E. D. Stokes, *Phys. Rev. A* **1**, 1424 (1970).

⁷J. S. Risley, F. J. de Heer, and C. B. Kerkdijk, *Abstracts of Papers of the Ninth International Conference on the Physics of Electronic and Atomic Collisions, Seattle, 1975* (University of Washington Press, Seattle, 1975), p. 93.

⁸J. S. Murray, S. J. Young, and J. R. Sheridan, *Phys. Rev. Lett.* **16**, 439 (1966).

⁹W. R. Hess, *Phys. Rev. A* **9**, 2036 (1974).